ELSEVIER

6 September 1996

Chemical Physics Letters 259 (1996) 347–355

CHEMICAL PHYSICS LETTERS

Optimized multiple-quantum magic-angle spinning NMR experiments on half-integer quadrupoles

Jean-Paul Amoureux [a], Christian Fernandez [a], Lucio Frydman [b,1]

[a] *Laboratoire de Dynamique et Structure des Matériaux Moléculaires C.N.R.S. U.R.A. 801, Université des Sciences et Technologies de Lille, F-59655 Villeneuve d' Ascq Cedex, France*

[b] *Department of Chemistry (M / C 111), University of Illinois at Chicago, Chicago, IL 60607-7061, USA*

Received 12 February 1996; in final form 21 May 1996

Abstract

It has been recently shown that second-order anisotropies can be removed from solid phase NMR spectra of quadrupolar nuclei via the combined use of magic-angle spinning (MAS) and bidimensional multiple-quantum (MQ) spectroscopy. The present study investigates the conditions under which the acquisition of such high-resolution MQMAS NMR spectra are optimized. The excitation and conversion pulse lengths that maximize $0 \rightarrow \pm 3(t_1) \rightarrow -1(t_2)$ coherence transfer pathway signals for arbitrary spin numbers were calculated, as were the pulse lengths that provide NMR spectra free from dispersive line shape distortions. For the case of spin-5/2 nuclei, the conditions which optimize experiments involving quintuple-quantum coherences were also determined.

1. Introduction

Quadrupolar nuclei with half-integer spin numbers $S(3/2, 5/2, 7/2, 9/2)$ constitute the single largest group of magnetically active nuclides in the Periodic Table [1]. Nuclear magnetic resonance (NMR) experiments performed on these nuclei in the solid phase are dominated by the usual coupling to the external magnetic field B_0, as well as by couplings between spins and their surrounding electric field gradients [2,3]. These quadrupolar interactions are often so strong that upon attempting NMR observations on powdered samples only the central $-1/2 \leftrightarrow +1/2$ transitions, which to first order are not affected by the quadrupolar Hamiltonian, remain observable. Signals arising from these transitions are still affected by second-order quadrupole effects [2]. Even under high-field NMR operation these interactions can be several tens of kHz strong, thereby complicating the interpretation of powder NMR spectra when dealing with samples possessing inequivalent chemical species.

An approach commonly employed to narrow these central transition resonances is magic-angle spinning (MAS), an experiment involving the fast rotation of samples at an angle $\beta = 54.7°$ with respect to B_0. Although this strategy is widely and successfully used in the spectroscopy of spin-1/2 for averaging out chemical shift and dipolar anisotropies [4,5], the reorientational symmetry that it involves is too low for canceling second-order quadrupolar anisotropies [6]. Generally speaking MAS only manages to reduce second-order quadrupolar broadenings by a fac-

[1] Camille and Henry Dreyfus New Faculty Awardee (1992–1997); Beckman Young Investigator (1996–1998).

PII S0009-2614(96)00809-3

tor of 3, a performance that may actually be improved by spinning the sample at angles other than the magic axis [7]. The elusive goal of retrieving truly isotropic solid state NMR spectra from half-integer quadrupoles was achieved thanks to the development of a novel theoretical framework, involving an expansion of second-order effects in terms of zero- (or isotropic), second- and fourth-rank spherical tensor components [8,9]. This theoretical approach crystallized in two different techniques, dynamic-angle spinning (DAS) and double rotation (DOR), that have gained a widespread attention owing to their promising chemical applications [10,11].

In spite of their success, the limitations of DAS in dealing with strongly dipole-coupled or fast-relaxing systems and the technical challenges posed by DOR, stimulated the search of alternative methods capable of yielding isotropic NMR spectra from half-integer quadrupoles. A solution to this challenge was recently achieved with the realization that multiple-quantum (MQ) MAS NMR can perform an averaging procedure similar to the one occurring in DAS, albeit via the combined use of spatial and spin manipulations [12]. In principle it would be natural to assume that the demands of this MQMAS methodology, involving the generation of multiple-quantum coherences within an ensemble possessing MHz-wide distributions of coupling constants, would constitute an unviable proposition. Nevertheless since its initial postulation, numerous examples of this methodology to important NMR probes such as ^{11}B, ^{17}O, ^{23}Na, ^{27}Al, ^{51}V, ^{55}Mn and ^{87}Rb have been demonstrated [12–20]. In view of the promise that this approach holds for the acquisition of high-resolution solid phase quadrupolar NMR spectra, we have embarked on a systematic effort to identify the conditions that should be adopted for performing this kind of experiment on arbitrary spins. The present paper presents some of the results stemming from these investigations.

2. MQMAS: theoretical background

The system that will be considered here consists of a powdered ensemble of half-integer quadrupolar nuclei subjected to the combined effects of Zeeman, shielding and quadrupolar interactions. We will assume that the first of these interactions is dominant, thereby allowing us to take into account the quadrupole interaction by considering its first- and second-order perturbative effects on the Zeeman eigenstates. This is a common situation in the NMR spectroscopy of a variety of nuclei [21], and leads to a rotating-frame spin Hamiltonian given by

$$\mathscr{H} = \mathscr{H}_q^{(1)} + \mathscr{H}_q^{(2)} + \mathscr{H}_{cs}, \tag{1}$$

where

$$\mathscr{H}_q^{(1)} = \tfrac{1}{2}\nu_q\left(3\cos^2\gamma - 1 + n_q \sin^2\gamma \cos 2\delta\right) \times \left[3S_z^2 - S(S+1)\right] \tag{2}$$

constitutes the secular component of the quadrupolar Hamiltonian depending on a coupling constant $\nu_q = (e^2qQ)/[4S(2S-1)h]$ and on an asymmetry parameter η_q,

$$\mathscr{H}_q^{(2)} = \left(\nu_q^2/\nu_0\right)\{R_{2,-1}R_{2,1}[T_{2,-1}, T_{2,1}] + R_{2,-2}R_{2,2}[T_{2,-2}, T_{2,2}]/2\} \tag{3}$$

describes the second-order quadrupole effects in terms of the spherical tensor elements $\{R_{2,m}, T_{2,m}\}$ and of the ratio between ν_q and the Larmor frequency ν_0, and

$$\mathscr{H}_{cs} = \nu_{cs}^{iso} S_z \tag{4}$$

represents the chemical shift interaction which for the sake of simplicity we shall assume is isotropic. The S_z^2-dependence of $\mathscr{H}_q^{(1)}$ implies that all NMR transitions between states differing in their $|S_z|$ value ($\pm 1/2 \leftrightarrow \pm 3/2$, $\pm 3/2 \leftrightarrow \pm 5/2$, etc.) will be affected by anisotropic first-order quadrupole effects proportional to ν_q, and thus lead to broad powder spectra of difficult observation and poor resolution. Due to this reason NMR experiments on quadrupolar nuclei have traditionally been confined to the observation of central $-1/2 \leftrightarrow +1/2$ transitions, which are only affected to second order by quadrupolar interactions. Initial attempts to average out the anisotropic frequency components in $\mathscr{H}_q^{(2)}$ focused on rapid macroscopic sample spinning at an angle β. The effects that these rotations have on $\mathscr{H}_q^{(2)}$ can be computed with the aid of Wigner rotation matrices

[22], which for symmetric $-m \leftrightarrow +m$ transitions lead to time-averaged precession frequencies [12,23]

$$\nu(S, m, \beta) = 2m\nu_{cs}^{iso} + \nu_q^{(0)} C_S^{(0)}(m) + \nu_q^{(2)}(\gamma, \delta) C_s^{(2)}(m) P_2(\cos\beta) + \nu_q^{(4)}(\gamma, \delta) C_S^{(4)}(m) P_4(\cos\beta), \quad (5)$$

where $\{C_S^{(l)}(m)\}_{l=0-4}$ are coefficients depending on the spin number S and on the Zeeman levels being correlated, and

$$P_2(\cos\beta) = (3\cos^2\beta - 1)/2, \quad (6a)$$

$$P_4(\cos\beta) = (35\cos^4\beta - 30\cos^2\beta + 3)/8 \quad (6b)$$

represent the second- and fourth-order Legendre polynomials. Due to the absence of common roots between these two polynomials, no single spinning axis can simultaneously cancel the anisotropic frequency terms in $\mathscr{H}_q^{(2)}$. One possible way of removing the (γ, δ)-dependence from this evolution consists of making β time-dependent. This approach underlies the DAS NMR technique, where initial and final spinning angles $\{\beta_1, \beta_2\}$ capable of fulfilling the refocusing conditions

$$P_2(\cos\beta_1)t_1 + P_2(\cos\beta_2)t_2 = 0, \quad (7a)$$

$$P_4(\cos\beta_1)t_1 + P_4(\cos\beta_2)t_2 = 0 \quad (7b)$$

are chosen throughout the course of a 2D correlation experiment. The recently proposed MQMAS technique achieves a similar bidimensional averaging by fixing the spinning axis at the magic angle ($P_2(\cos\beta) = 0$), while correlating the spin evolution between two different $\{-m_i \leftrightarrow +m_i\}_{i=1,2}$ coherence orders. Since symmetric transitions of this type are not affected by first-order quadrupole effects, all anisotropies will vanish at times (t_1, t_2) fulfilling the refocusing condition

$$C_S^{(4)}(m_1)t_1 + C_S^{(4)}(m_2)t_2 = 0. \quad (8)$$

The practical implementation of this 2D strategy demands acquiring the signal as a function of t_2, thus circumscribing m_2 to the central single-quantum transition. The value of m_1 as well as the apparent sense of precession during t_1, however, can be freely selected from within the spin manifold by applying the standard rules of phase cycling. It is then easy to verify that a triple-/single-quantum MAS correlation experiment can always provide a refocusing of the anisotropies, provided that the apparent sense of spin precession is kept constant for the $S = 3/2$ case and reversed for the remaining $S = 5/2, 7/2, 9/2$ cases [12]. When this refocusing occurs the signal arising from the spin ensemble will only depend on a linear combination of isotropic quadrupole and chemical shifts, and consequently its Fourier transformation will provide highly resolved NMR spectra even in the case of powdered samples.

It follows from these considerations that in its most basic form, MQMAS requires the generation of substantial amounts of triple-quantum coherences followed by their efficient transfer to the central $-1/2 \leftrightarrow +1/2$ transition. There are basically two procedures that can be used for implementing such an experiment: the three-pulse approach of the kind usually employed in isotropic systems [24]

$$(\tau_1)_{\phi_1} - \Delta(\text{MQ pumping}) - (\tau_2)_{\phi_2} - t_1 - (\tau_3)_{\phi_3} - t_2(\phi_{Rx}), \quad (9)$$

where τ_i represents the duration of an rf pulse and ϕ_i its relative phase, or the two-pulse approach [25–29]

$$(\tau_1)_{\phi_1} - t_1 - (\tau_2)_{\phi_2} - t_2(\phi_{Rx}) \quad (10)$$

specifically designed for operating on anisotropic couplings such as those encountered in solid or liquid-crystalline phases. Both sequences have already been successfully employed in the acquisition of MQMAS spectra; the latter approach, however, has been shown to yield consistently higher S/N ratios [14–16], and is thus the focus of the present investigation. The following paragraph describes in detail the conditions under which the sequence in Eq. (10) can yield MQMAS NMR spectra with optimized S/N ratios and purely absorptive line shapes for arbitrary spin numbers.

3. Manipulation of triple-quantum spin coherences

Analyzing the details of the triple-quantum excitation and its subsequent conversion to single-quantum

coherences on a random powder requires propagating the spin density matrix ρ under the effects of a non-commuting Hamiltonian containing quadrupolar, shielding and rf components, which are in turn rendered time-dependent due to the effects of sample spinning. These complex numerical calculations were carried out in the present study on a personal computer using the PULSAR simulation program, presented elsewhere in detail [30]. For the sake of simplicity, we began by analyzing the triple-quantum excitation in a powdered sample subject to the effects of a first-order quadrupolar Hamiltonian $\mathscr{H}_q^{(1)}$ and of an rf interaction

$$\mathscr{H}_{rf} = \nu_{rf} S_x. \tag{11}$$

Fig. 1 illustrates the build up of triple-quantum elements that for this case can be expected as a function of the initial excitation angle

$$\theta_1 = 360° \cdot \nu_{rf} \tau_1, \tag{12}$$

together with supporting experimental data collected on different model compounds. Since vertical scales in Fig. 1 are normalized to a maximum signal intensity of $-1/2 \leftrightarrow +1/2$ transitions equal to 1, these curves indicate that the single pulse excitation of apparently forbidden $-3/2 \leftrightarrow +3/2$ transitions can exceed by over 50% the amount of signal arising from central transitions. These curves also reveal an underlying similarity between the excitation profiles undergone by different spins, which becomes apparent once the $2S+1$ factor that scales the nutation rate of quadrupolar nuclei is taken into account. Thus spin-3/2 curves reveal broad local maxima for nutation angles θ_1 in the neighborhood of 240°, which sharpen and shift towards lower values as the spin number increases. For $S = 5/2$ triple-quantum coherences reach an initial local maximum for $\theta_1 \approx 180°$ over a range of ν_q/ν_{rf} ratios; for $S = 7/2$ and $S = 9/2$ excitation pulses of 120° and 90° seem appropriate choices for MQMAS experiments involving moderate quadrupolar coupling constants and conventional rf field strengths.

Investigations were also carried out in order to determine the conditions that maximize the conversion of the triple-quantum coherences evolving during t_1, into the central single-quantum coherences to be detected. In contrast to what happened in the case

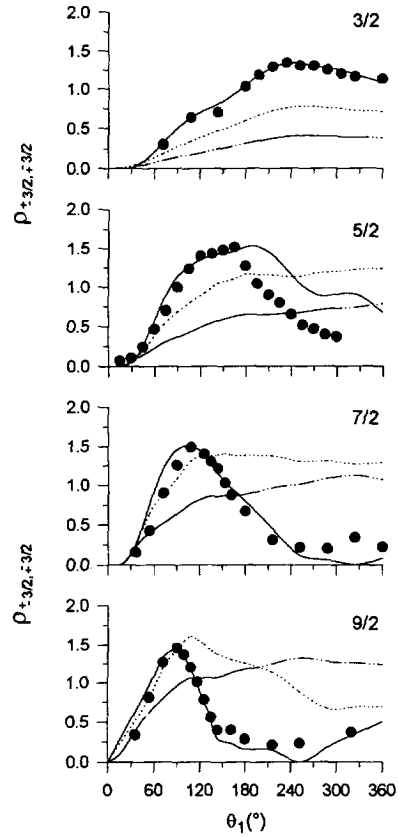

Fig. 1. Build up curves for the generation of triple-quantum coherences in a powdered sample, calculated for the indicated spin numbers as a function of the pulse angle θ_1. Computations assumed the following ratios between ν_q and ν_{rf} ($\eta_q = 0$): $\nu_q/\nu_{rf} = 5$ (–···–), $\nu_q/\nu_{rf} = 2.5$ (···), $\nu_q/\nu_{rf} = 1.25$ (—). Black dots correspond to experimental data collected for the latter ratio on $^{23}Na_2SO_4$ ($S = 3/2$), $K^{55}MnO_4$ ($S = 5/2$), $K_3{}^{59}Co(CN)_6$ ($S = 7/2$) and $Li^{93}NbO_3$ ($S = 9/2$) samples. These measurements were carried out at 9.4 T using a Bruker ASX-400 NMR spectrometer and MAS probehead, and subsequently normalized to match the theoretical profiles.

of the excitation, where signal optimization simply involved determining the conditions that yield the largest $\rho_{\pm 3/2,\mp 3/2}$ elements starting from an initial Boltzman equilibrium condition $\rho_0 \propto S_z$, maximizing the coherence transferred into the central transition requires dealing with two different initial states: $\rho_0 = \rho_{+3/2,-3/2}$ and $\rho_0 = \rho_{-3/2,+3/2}$. Since the fate of each of these two elements upon rf irradiation is different, the signal intensities arising from $0 \rightarrow -3(t_1) \rightarrow -1(t_2)$ and $0 \rightarrow +3(t_1) \rightarrow -1(t_2)$ coher-

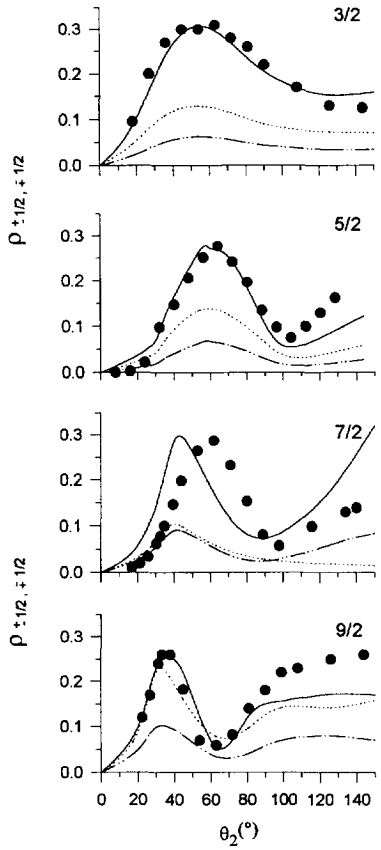

Fig. 2. Dependence of triple- to single-quantum coherence transfer processes on the rf pulse angle θ_2, calculated (curves) and measured (dots) for the indicated spin numbers. Investigations focused on the $0 \rightarrow -3(t_1) \rightarrow -1(t_2)$ transfer pathway for $S = 3/2$ and on $0 \rightarrow +3(t_1) \rightarrow -1(t_2)$ for the remaining spins, and employed initial excitation pulses $\theta_1 = 240°$ ($S = 3/2$), 180° ($S = 5/2$), 120° ($S = 7/2$) and 90° ($S = 9/2$). Other computational and experimental conditions are as in Fig. 1.

ence transfer pathways upon application of a final conversion pulse

$$\theta_2 = 360° \cdot \nu_{rf} \tau_2 \qquad (13)$$

will differ. As mentioned above, the first of these pathways will refocus second-order quadrupolar anisotropies for $S = 3/2$ while the latter will refocus anisotropies for nuclei with spin $S \geqslant 5/2$. Our investigations were therefore restricted to the optimization of the triple- to single-quantum conversion process for these coherence transfer and spin number combinations. Fig. 2 illustrates theoretical and experimental conversion profiles resulting for a series of ν_q/ν_{rf} and S values. As happened in the case of the triple-quantum excitation, these curves reveal well-defined nutation angles θ_2 capable of maximizing the desired conversion over a range of ν_q/ν_{rf} ratios; these values are 55° for $S = 3/2$, 60° for $S = 5/2$, 45° for $S = 7/2$ and 35° for $S = 9/2$. By contrast to what we observed in the excitation, however, these calculations show that the triple- to single-quantum conversion is a fairly inefficient process which can be expected to limit S/N ratios in MQMAS NMR.

A trend which can be noticed from the data shown in Figs. 1 and 2 is that within usual ranges of ν_q/ν_{rf} ratios, the smaller this parameter becomes the more efficient the excitation and conversion processes involved in MQMAS can be made. We decided to further investigate this issue by computing the maximum amount of observable single-quantum coherence that can be generated by a two-pulse MQMAS experiment as a function of ν_q/ν_{rf}. As above, our attention focused on the $0 \rightarrow -3(t_1) \rightarrow -1(t_2)$ coherence transfer pathway for $S = 3/2$ and on $0 \rightarrow +3(t_1) \rightarrow -1(t_2)$ for the remaining spin

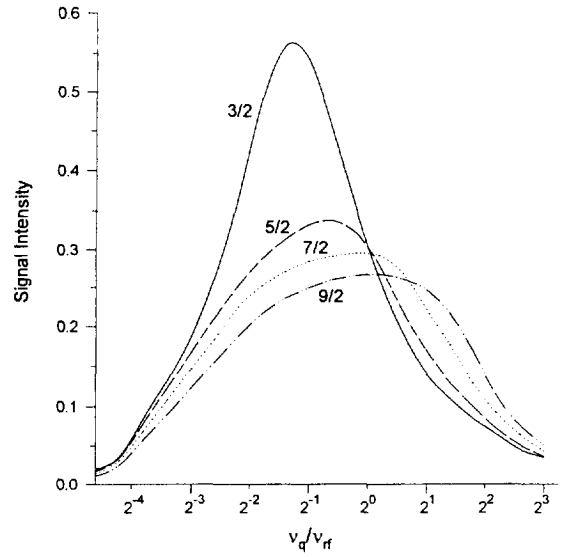

Fig. 3. Dependence of the maximum signal observable in MQMAS on the ν_q/ν_{rf} ratio for different spin numbers. For all spins the maximum signal intensity that can be expected from ideal central transition experiments is normalized to 1, and no asymmetry parameters, chemical shifts or second-order effects were considered. The (θ_1, θ_2) pulse angles employed in these calculations were (240°, 55°) ($S = 3/2$), (180°, 60°) ($S = 5/2$), (120°, 45°) ($S = 7/2$), (90°, 35°) ($S = 9/2$).

numbers. The results of these calculations are presented in Fig. 3. Even for the moderately large rf field strengths currently available (50–120 kHz) the regions of interest in these curves are located to the right of the observed maxima, as the portions on the left correspond to small ν_q values whose second-order effects are small and amenable to averaging by conventional MAS. These data evidence that increasing the rf field strength can have a dramatic effect on the signal available during MQMAS acquisitions, and reductions of up to an order of magnitude in the total acquisition time can be achieved by doubling ν_{rf}. Also interesting to note is the monotonic decrease in maximum detectable signal that these plots evidence with increasing spin number; MQMAS signal intensities decay from $\approx 55\%$ of the maximum central transition signal for optimized spin-3/2 acquisitions to only 25% for the $S = 9/2$ case.

Also worth analyzing is the relative efficiency with which for a given spin number, individual $\rho_{-3/2,+3/2}$ and $\rho_{+3/2,-3/2}$ coherences are converted into single-quantum observables by the effects of the final θ_2 pulse. Although only one of these elements will experience an isotropic second-order refocusing, the need for acquiring both echo and anti-echo coherence transfer pathway signals arises when trying to obtain bidimensional isotropic–anisotropic MQMAS correlation spectra that are completely free from dispersive components. As is known, calculation of purely absorptive 2D NMR spectra requires the collection of equally strong signals from both coherence pathways either simultaneously, leading to amplitude-modulated data, or sequentially, leading to hypercomplex-type sets [31]. Even though MQMAS is by design an echo experiment and therefore possesses relatively minor dispersive distortions even if only one coherence transfer pathway is monitored, acquisition of equalized echo and anti-echo signals can be of considerable aid when dealing with broad bidimensional resonances such as those expected from glasses. In consequence we investigated the possibility of making the signals arising from echo and anti-echo pathways identical by using as a variable the nutation angle θ_2. Fig. 4A illustrates both theoretically and experimentally, the effects that changing the duration of this triple-/single-quantum conversion pulse introduces on the relative intensities of the two spin-3/2 coherence transfer pathways. A crossing point of both pathways can be observed at $\theta_2 = 90°$, a value that is longer than the one that maximized the overall spectral S/N. Noteworthy the equalization in pathway intensities occurring under these conditions does not merely reflect an average over the powdered sample, but is actually a phenomenon that occurs for every single-crystallite regardless of its orientation. This θ_2 condition will therefore lead to purely-absorptive MQMAS line shapes over the complete 2D spectral powder pat-

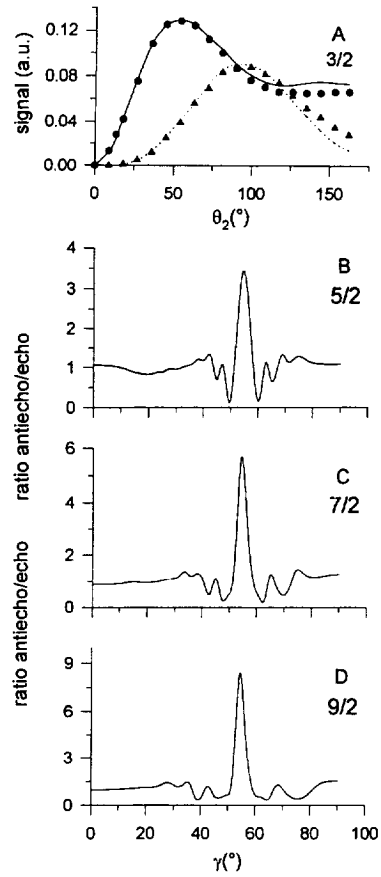

Fig. 4. (A) Comparison between the total echo (—) and anti-echo (– – –) signal intensities calculated for a spin-3/2 powder as a function of the θ_2 pulse angle. Points in the graph correspond to ^{23}Na MQMAS NMR data collected at 105.8 MHz on a Na_2SO_4 sample. (B)–(D) Orientation dependence of the ratio between the anti-echo and echo signals for $S = 5/2$, 7/2 and 9/2 spins on the angle γ defined in Eq. (2). $\mathscr{K}_q^{(2)}$, $\mathscr{K}_{cs}$ and η_q were assumed zero; θ_2 nutation angles were chosen to minimize the differences between the two pathways intensities ($\theta_2 = 56°$ for $S = 5/2$, 42° for $S = 7/2$, 33° for $S = 9/2$).

tern. This is in contrast to what is found upon analyzing nuclei possessing higher spin numbers, for which no condition is capable of equalizing the intensities of echo and anti-echo pathways simultaneously for all crystallites in the sample (Figs. 4B–4D). The deviation from the ideal anti-echo/echo ratio of 1 actually increases with spin number, thus making it impossible to retrieve MQMAS spectra that are free along both spectral dimensions of at least minor dispersive artifacts.

4. Offset-induced distortions in MQMAS NMR

The analyses of the preceding section assumed that the only interactions affecting the spin ensemble were the Zeeman coupling, the first-order component of the quadrupolar Hamiltonian and the on-resonance irradiation $\mathscr{H}_{rf}$. Under this assumption an initial excitation pulse along the x axis transforms the equilibrium S_z magnetization into purely imaginary (S_y) triple-quantum coherences, and the final conversion pulse transforms these triple-quantum coherences into purely imaginary single-quantum observables. In real systems, however, additional evolution takes place during the excitation and conversion pulses due to the second-order quadrupolar and chemical shielding interactions. An analysis of the effects introduced by $\mathscr{H}_{cs}$ reveals that although both the amplitude and phase of the final spectral peaks will be affected by this interaction, these distortions will be minor for offsets fulfilling $|\nu_{cs}^{iso}| \leqslant \nu_{rf}/5$. Larger shielding offsets will start to play an important role in the signal intensity, but their phase distortions can still be dealt with using conventional zero- and first-order phase corrections. Calculations show that this will not be the case for second-order quadrupole effects, whose phase distortions cannot be compensated by a simple linear frequency correction.

5. MQMAS using quintuple-quantum coherences

So far this discussion has been circumscribed to the acquisition of MQMAS spectra arising from $0 \rightarrow \pm 3(t_1) \rightarrow -1(t_2)$ coherence transfer pathways. The main reason for focusing exclusively on triple-quantum experiments is their general applicability, and their ability to provide MQMAS spectra possessing the highest S/N ratios. It is conceivable, however, that in the study of certain systems involving nuclei with $S \geqslant 5/2$, it might be desirable to trade part of this signal for the sake of an improved spectral resolution by monitoring higher orders of coherence. Isotropic chemical shift separations will always increase with order, as they are simply proportional to m_1. The isotropic quadrupolar evolution may also be magnified by increasing m_1; for a spin-5/2 for instance this shift will have increased by the time of the anisotropic refocusing from a value of $2.6\nu_q^{(0)}$ for a $0 \rightarrow \pm 3(t_1) \rightarrow -1(t_2)$ experiment, to $10.8\nu_q^{(0)}$ for a $0 \rightarrow \pm 5(t_1) \rightarrow -1(t_2)$ correlation. Although these considerations do not factor in the relative signs of the chemical and quadrupolar shifts, which may or may not oppose one another, it is clear that a five-quantum MQMAS NMR experi-

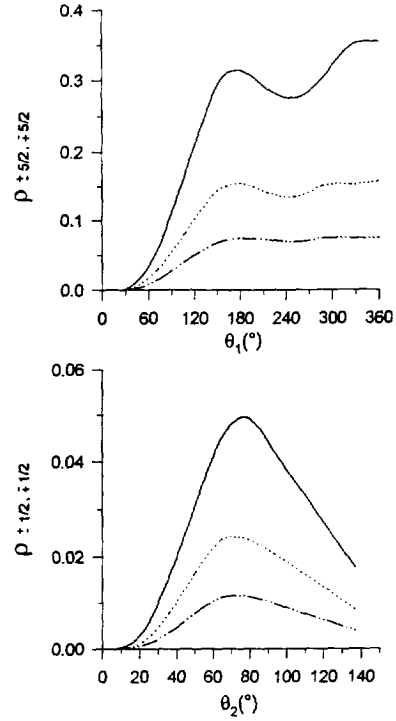

Fig. 5. Dependence of the excitation (top) and single-quantum conversion (bottom) processes for a quintuple-quantum MQMAS experiment on a spin-5/2 nucleus as a function of the nutation angles θ_1 and θ_2. Calculations were carried out using the same assumptions and definitions as in Fig. 1.

ment on $S = 5/2$ will in general have a higher resolution than its triple-quantum counterpart. We decided therefore to investigate for the case $S = 5/2$ the conditions that maximize the excitation of quintuple-quantum coherences by effects of a single pulse, as well as their subsequent conversion to observable $\rho_{-1/2,+1/2}$ elements by application of a final mixing pulse. Fig. 5 summarizes the results of these calculations for typical values of ^{17}O or ^{27}Al quadrupolar coupling parameters. These plots reveal optimum pulse widths for quintuple-quantum experiments corresponding to $\theta_1 \approx 170°$, $\theta_2 \approx 70°$ over a range of ν_q/ν_{rf} values. Still, even under these optimized conditions, the signal intensities that can be expected from these spectra amount to less than 20% of the value that they reached in the optimized triple-quantum MQMAS acquisitions.

6. Conclusions

The present work introduced optimized experimental parameters for the acquisition of MQMAS NMR data on different spins. These results should help expand the use of this new methodology, simplifying its application to a growing range of chemical materials. Still it is worth noting that the parameters that were hereby presented will yield optimized spectra only under ideal conditions, and are expected to be somewhat dependent on the particular characteristics of the actual sample under analysis. This dependence may be particularly important upon operating with strong rf fields in excess of 100 kHz, when changes of only a fraction of a microsecond can introduce considerable variations in the magnitude of the final signal. It is consequently advisable to regard the conditions that are here discussed as best initial setup parameters for a given spin number, susceptible to improvement by virtue of minor manipulations.

Acknowledgement

We are grateful to Professors J. Virlet (Paris) and D. Massiot (Orléans) for helpful discussions. Technical support for this work was received from Bruker (Karlsruhe). Financial support was received from CNRS (JPA and CF) and from the US National Science Foundation through grants DMR-9420458 and CHE-9502644 (LF).

References

[1] R.K. Harris and B.E. Mann, NMR and the Periodic Table (Academic Press, New York, 1970).
[2] A. Abragam, The principles of nuclear magnetism (Oxford Univ. Press, London, 1985).
[3] C.P. Slichter, Principles of nuclear magnetic resonance (Springer, Berlin, 1990).
[4] E.R. Andrew, A. Bradbury and R.G. Eades, Nature 182 (1958) 1659.
[5] I.J. Lowe, Phys. Rev. Lett. 2 (1959) 285.
[6] F. Lefebvre, J.-P. Amoureux, C. Fernandez and E.G. Derouane, J. Chem. Phys. 86 (1987) 6070.
[7] S. Ganapathy, S. Schramm and E. Oldfield, J. Chem. Phys. 77 (1982) 4360.
[8] A. Llor and J. Virlet, Chem. Phys. Lett. 152 (1988) 248.
[9] E.W. Wooten, K.T. Muller and A. Pines, Acc. Chem. Res. 25 (1992) 209.
[10] B.F. Chmelka, K.T. Mueller, A. Pines, J. Stebbins, Y. Wu and J.W. Zwanziger, Nature 339 (1989) 42.
[11] K.T. Mueller, B.Q. Sun, G.C. Chingas, J.W. Zwanziger, T. Terao and A. Pines, J. Magn. Reson. 86 (1990) 470.
[12] L. Frydman and J.S. Harwood, J. Am. Chem. Soc. 117 (1995) 5367.
[13] M.J. Duer and C. Stourton, Poster WP222 in 35th ENC, Pacific Grove, California (1994).
[14] C. Fernandez and J.-P. Amoureux, Chem. Phys. Lett. 242 (1995) 449.
[15] A. Medek, J.S. Harwood and L. Frydman, J. Am. Chem. Soc. 117 (1995) 12779.
[16] G. Wu, D. Rovnyak, B. Sun and R.G. Griffin, Chem. Phys. Lett. 249 (1995) 210.
[17] D. Massiot, B. Tonzo, D. Trumean, J.P. Coutures, J. Virlet, P. Florian and P.J. Grandinetti, Solid State NMR 6 (1996) 73.
[18] C. Fernandez and J.-P. Amoureux, Solid State NMR 5 (1996) 315.
[19] R.E. Youngman, U. Werner-Zwanziger and J.W. Zwanziger, Z. Naturforsch., in press.
[20] C. Fernandez, J.-P. Amoureux, H. Kessler and L. Delmotte, Microporous Mater., in press.
[21] P. Granger and R.K. Harris, eds. Multinuclear magnetic resonance in liquids and solids – chemical applications (Kluwer, Dordrecht, 1990).
[22] U. Haeberlen, Advances in magnetic resonance, Suppl. 1 (Academic Press, New York, 1976).
[23] J.-P. Amoureux, Solid State NMR 2 (1993) 83.
[24] G. Bodenhausen, Prog. Nucl. Magn. Reson. Spectrosc. 14 (1981) 137.

[25] S. Vega and A. Pines, J. Chem. Phys. 66 (1977) 5624.
[26] A. Wokaun and R.R. Ernst, J. Chem. Phys. 67 (1977) 1752.
[27] S. Vega, J. Chem. Phys. 68 (1978) 5518.
[28] S. Vega and Y.J. Naor, J. Chem. Phys. 75 (1981) 75.
[29] N.C. Nielsen, H. Bildsøe and H.J. Jakobsen, Chem. Phys. Lett. 191 (1992) 205.
[30] J.-P. Amoureux, C. Fernandez and Y. Dumazy, J. Chim. Phys. 2 (1995) 1939.
[31] R.R. Ernst, G. Bodenhausen and A. Wokaun, Principles of nuclear magnetic resonance in one and two dimensions (Clarendon Press, Oxford, 1987).